Control excitation and coherent transfer in a dimer

Hong-rong Li,[1,*] Pei Zhang,[1,*] Yingjun Liu,[2] Fu-li Li,[1] and Shi-yao Zhu[3]
[1]*Department of Applied Physics, Xian Jiaotong University, Xian 710049, China*
[2]*The High School Affiliated to Xi'an Jiaotong University, Xian 710054, China*
[3]*Beijing Computational Science Research Center, Beijing 100084, China*
(Received 2 March 2013; published 24 May 2013)

In this article, the processes of energy absorption and coherent transfer in a dimer are studied. The dimer includes two two-level pigments, donor and acceptor, where the donor is assumed to be excited by a control pulse in the time domain. We investigate the dynamics of probability that the acceptor is in the excited state and the total efficiency of energy absorption and transfer under different temporal shapes of the control pulse. Quantum concurrence of the dimer is also discussed.

DOI: 10.1103/PhysRevA.87.053831 PACS number(s): 42.50.Ct, 71.35.−y, 03.65.Ud, 03.65.Yz

I. INTRODUCTION

The primary processes in photosynthesis have been paid much interest [1–7] from the broader physical community in recent years, thanks to experimental observation via electronic spectroscopy technology [8] demonstrating that quantum coherence is involved in the excitation energy transfer of the light-harvesting complexes [3] and Fenna-Matthews-Olson complex [9]. In most of the photosynthetic processes, photochemical excitation of an antenna molecule by absorbing a pulse of light takes place first, and the absorbed excitation energy is then transferred among molecules of the photosynthetic systems until reaction centers where the energy is converted into chemical energy [1–3].

According to the Förster theory [10], when the electronic coupling between pigments is small in comparison to the electron-environment coupling, the energy transfer between different pigments takes place through incoherent hopping, where the electronic coupling can be treated perturbatively. On the contrary, when the electronic coupling between pigments is similar or larger than the reorganization energy of the pigments, electronic excitations then move coherently through different pigments rather than by incoherent hopping motion [11]. In the later case, the electron-environment coupling can be treated perturbatively to obtain a quantum master equation [12]. Recent experimental [13–17] and theoretical works [18–39] support the coherent transfer case and indicate that long-lasting electronic coherence can indeed influence the excitation-transfer dynamics in photosynthetic complexes. The process of energy transfer takes only a few hundred picoseconds and is performed with extraordinarily high efficiency [3]. In most of the above theoretical works, investigation has been focused only on the energy-transfer processes, with the assumption that the initial pigments are in their excited states. However, this assumption is possible only when the shape of light pulses is very sharp, i.e., nearly a δ-function pulse. In this situation, the process of light absorption occurs rapidly before excitation energy transferring starts. In fact, the shape of the pulses that antenna molecules absorb may have temporal width, which means that the processes of energy transferring always take place at the same time with the processes of absorbing light pulses. Therefore it is necessary to consider the effects of the shape of pulses on efficiency of energy transfer. This is the key motivation of our present work.

To investigate how the shape of light pulses affects the processes of energy absorption and transferring, instead of considering a complicated network of pigments where the practical transfer processes take place, we will study a basic physical part to obtain the physical mechanism: a dimer system which consists of a donor pigment and an acceptor pigment modeled by two two-level systems. With the assumption that the two pigments are both in their ground states initially, we will study the dynamics of the dimer system after the donor pigment is excited by a light pulse and absorbs the energy of light. The efficiency of the energy absorption and transfer will be discussed by calculating the probabilities of the acceptor pigment in its upper state. Our study is suitable for quantum control settings under artificial laser light conditions. The previous studies in molecular dimers and excitation with coherent pulses can be found in [40,41].

The paper is organized as follows. In Sec. II, a theoretical model and simple analyses are presented. In Sec. III, numerical results are shown. Conclusions and final remarks are presented in Sec. IV.

II. THE THEORETICAL MODEL AND THE ASSOCIATED DYNAMICS

The free Hamiltonian of the two pigments is

$$H_1 = \tfrac{1}{2}\omega_1\sigma_z^{(1)} + \tfrac{1}{2}\omega_2\sigma_z^{(2)}, \tag{1}$$

and the coupling Hamiltonian between the two pigments is given by

$$H_2 = J(\sigma_+^{(1)}\sigma_-^{(2)} + \sigma_-^{(1)}\sigma_+^{(2)}), \tag{2}$$

where ω_i represents energy separation of the ith pigment, J is the coupling strength, and $\sigma_z^{(i)} = |e\rangle_i\langle e| - |g\rangle_i\langle g|$ is the Pauli operator for the ith pigment; $\sigma_+^{(i)} = |e\rangle_i\langle g|$ and $\sigma_-^{(i)} = |g\rangle_i\langle e|$ are the arising and lowering operators for the ith pigment, respectively. If we assume that the donor pigment is excited by an external pulse, the associated Hamiltonian is

$$H_3 = E(t)\sigma_+^{(1)} + E^*(t)\sigma_-^{(1)}, \tag{3}$$

where $E(t) = E_\Omega(t)e^{i\Omega t}$ is a time-dependent amplitude of the external pulse. For example, for the Gaussian-type laser pulse, $E_\Omega(t) = \frac{E_0}{\sqrt{2\pi}\tau_p}e^{-t^2/2\tau_p^2}$, and τ_p is the FWHM of the pulse.

*hrli@mail.xjtu.edu.cn, zhang.pei@mail.xjtu.edu.cn

H_1, H_2, and H_3 are the Hamiltonian of the two-level system, which can be simply denoted by $H_M = H_1 + H_2 + H_3$. In real photosynthetic systems, the effect of noise from the environment (e.g., vibrational modes of protein molecules in the environment) is unavoidable. Here, we naturally use a Bose bath to denote the environmental modes, and the coupling Hamiltonian of the system and the environmental modes is

$$H_{MB} = \sum_{j=1}^{2} \sigma_z^{(j)} \sum_{k_j} g_{kj}\left(a_{k_j}^{\dagger} + a_{k_j}\right), \tag{4}$$

where $a_{k_j}^{\dagger}$ is the creation operator of the Bose bath with mode k_j, and g_{k_j} is the coupling strength between the jth pigment and the mode k_j of the bath. The free Hamiltonian of the bath is

$$H_B = \sum_{k_j} \nu_{k_j} a_{k_j}^{\dagger} a_{k_j}, \tag{5}$$

where ν_{k_j} represents the frequency of the mode k_j.

To get the evolution of the system, we first write the Hamiltonian into its eigenspace. The eigenequation of the systems is given by $H_M|\epsilon_j\rangle = \epsilon_j|\epsilon_j\rangle$, where $|\epsilon_j\rangle$ is the corresponding eigenvector for the jth eigenvalue ϵ_j. With solving the corresponding secular equation $|H_M - \epsilon I| = 0$, we obtain the four eigenvalues $\epsilon_{1,2} = \mp\frac{1}{2}\sqrt{\varepsilon_1 + 2\varepsilon_0}$, $\epsilon_{3,4} = \pm\frac{1}{2}\sqrt{\varepsilon_1 - 2\varepsilon_0}$, where $\varepsilon_0 = \sqrt{4|E|^2(J^2+\omega_2^2) + (J^2 - \omega_1\omega_2)^2}$, and $\varepsilon_1 = 2J^2 + 4|E|^2 + \omega_1^2 + \omega_2^2$. We notice that $\epsilon_2 \geqslant \epsilon_3 \geqslant \epsilon_4 \geqslant \epsilon_1$. For each eigenvalue ϵ_i, the corresponding eigenvector $|\epsilon_i\rangle$ is a linear superposition of the four bare states $|\eta_1\rangle = |ee\rangle$, $|\eta_2\rangle = |eg\rangle$, $|\eta_3\rangle = |ge\rangle$, and $|\eta_4\rangle = |gg\rangle$ of the two-level system. If we let $|\epsilon\rangle = [|\epsilon_1\rangle, |\epsilon_2\rangle, |\epsilon_3\rangle, |\epsilon_4\rangle]^T$, and $|\eta\rangle = [|\eta_1\rangle, |\eta_2\rangle, |\eta_3\rangle, |\eta_4\rangle]^T$, and use $U = \{u_{ij}\}$ to denote the transform matrix from $|\epsilon\rangle$ to $|\eta\rangle$, then we have a simple form between the original state vectors and the eigenstate vectors,

$$|\eta\rangle = U|\epsilon\rangle. \tag{6}$$

In the eigenspace, the diagonal form of the Hamiltonian is

$$H_M = \sum_{i=1}^{4} \epsilon_i |\epsilon_i\rangle\langle\epsilon_i|. \tag{7}$$

In the new basis, the Pauli operators $\sigma_z^{(m)} = |e\rangle_m\langle e| - |g\rangle_m\langle g| = \sum_{i,j=1}^{4} s_{ij}^{(m)}|\epsilon_i\rangle\langle\epsilon_j|$, where $s_{ij}^{(1)} = u_{1i}u_{1j}^* + u_{2i}u_{2j}^* - u_{3i}u_{3j}^* - u_{4i}u_{4j}^*$ and $s_{ij}^{(2)} = u_{1i}u_{1j}^* - u_{2i}u_{2j}^* + u_{3i}u_{3j}^* - u_{4i}u_{4j}^*$. Using these notations, we rewrite the coupling Hamiltonian as

$$H_{MB} = \sum_{l=1}^{2}\sum_{k_l}\sum_{i,j=1}^{4} s_{ij}^{(l)} g_{k_l} |\epsilon_i\rangle\langle\epsilon_j|\left(a_{k_l}^{\dagger} + a_{k_l}\right). \tag{8}$$

To give an elementary view of the dynamics of our model, we first consider a closed evolution based on the H_M. With assuming that the two pigments are both in their ground states initially, $|\varphi(0)\rangle = |gg\rangle = |\eta_4\rangle = \sum_{j=1}^{4} u_{4j}(0)|\epsilon_j\rangle$, and after applying to the Schrödinger equation, we have the formal solution of the system $|\varphi(t)\rangle = e^{-i\int H_M(t)dt}|\varphi(0)\rangle$. We consider two extreme cases: $J^{-1} \gg \tau_p$ and $J^{-1} \ll \tau_p$.

In the first case of $J^{-1} \gg \tau_p \to 0$, the input pulse is a sharp wave packet, because $a \to 0$, $\frac{1}{a\sqrt{\pi}}e^{-x^2/a^2} \to \delta(x)$. This means that for the Gaussian-type pulse, $E_\Omega(t) \to E_0\delta(t)$ with $\sqrt{2}\tau_p \to 0$. We thus suppose that the whole dynamic process has two steps: (1) the donor pigment is excited by the input pulse; and (2) excitation energy transfers from the donor to the acceptor. In the first step, we find $H_M \approx H_3$ as $E(t) \sim \delta(t)$; thus we have the dynamic states at time t_1 after the pulse takes action, $|\psi(t_1)\rangle = e^{-i\int_0^{t_1} H_3(t')dt'}|gg\rangle = e^{i\gamma_0}|eg\rangle$. After the action of $\delta(t)$ pulse, as $E(t) \sim 0$, we have $H_M \approx H_1 + H_2$, which corresponds to the second step, i.e., energy transferring from the donor pigment to the acceptor pigment starts when the donor pigment is in its excited state, which is also the common assumption in some of the published works about quantum dynamics of photosynthesis [28–33].

The second extreme case associates to a near flat and continuous action pulse, with assuming simply that $E(t) \sim E_c$. We then find that $|\psi(t)\rangle \approx \sum_{j=1}^{4} u_{4j}(0)e^{-i\epsilon_j t}|\epsilon_j\rangle$. Normally, the shape of a pulse absorbed by an antenna molecule is not sharp—the pulse has width in the space and time domain. Spatial and temporal coherence, and other effects coming from its shape, should be considered, and the process of excitation transfer is surely affected by these effects because the spatial and temporal width of a control pulse is similar to the space and time scale in excitation transfer processes [13–17]. On the one hand, as the wave packet of the photons captured by antenna pigments is always larger than or comparable to the scales of multichromophoric molecules [6], the initial excitation takes place coherently among the antenna pigments. Thus the efficiency of energy transferring from the antenna to the reaction center depends intimately on the quantum superposition properties of the initial states [18], and this initial spatial coherence will enhance or trap transfer of the donor pigments at different conditions [18–22]. Similarly, on the other hand, under a single excitation assumption, a pulse with temporal width will induce excitation coherent at different times, i.e., with different phase, the temporal shape of an input pulse can also affect processes of excitation transfer. For example, in a process of absorbing and transferring energy with a flat input pulse, the donor is first excited from $|gg\rangle$ to $|eg\rangle$ by the front part of the input pulse, and then coupling between two pigments induces excitation transfer from $|eg\rangle$ to $|ge\rangle$; the next part of the pulse will then coherently stimulate the pigments from $|gg\rangle$ to $|eg\rangle$ and from $|ge\rangle$ to $|ee\rangle$. This means the donor is then always in its excited states, which will lead to saturation of energy absorbing and transferring, thus increasing dissipation and reducing efficiency. Therefore, in a more realistic pulse-absorbing process of photosynthesis, one needs to not only consider efficiency of energy transfer between different pigments, but also investigate the whole efficiency, including pulse energy absorption. To investigate the whole efficiency including pulse energy absorption and energy transfer from the donor to the acceptor, we directly use the area under the pulse figure in the time domain to denote the total power of the pulse, and define a parameter of total efficiency as follows:

$$\eta_{\text{total}} = \frac{\omega_2 \text{Tr}[|e\rangle_2\langle e|]}{\int |E(t)|^2 dt}. \tag{9}$$

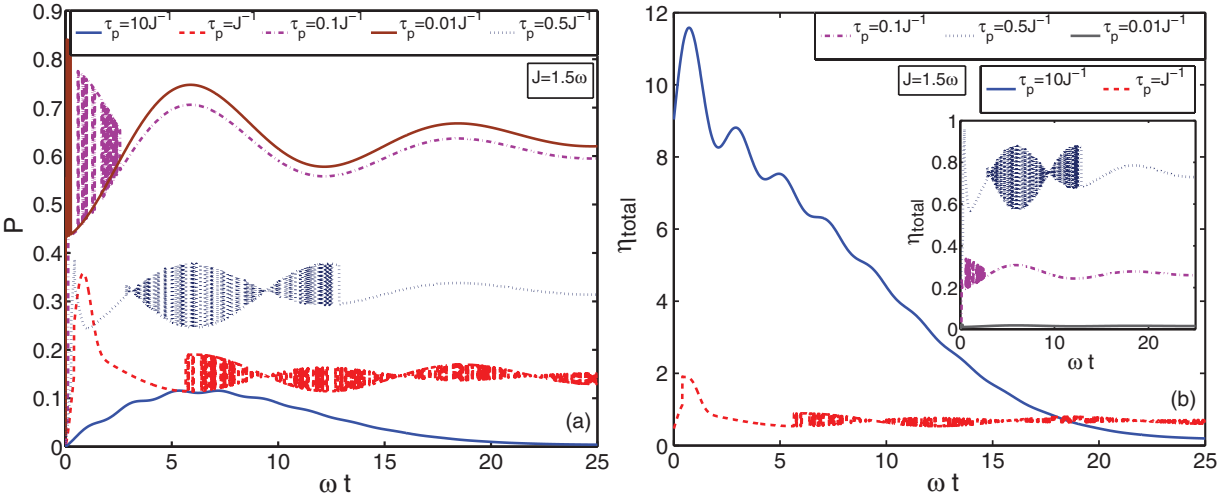

FIG. 1. (Color online) Probability P that the acceptor is in the excited state and the parameter of total efficiency η_{total} versus time ωt are plotted. We set $\omega_1 = \omega_2 = \omega$, $J = 1.5\omega$, $\kappa_1 = \kappa_2 = 0.1\omega$, $T_1 = T_2 = 0.1\omega$. The same parameters are also chosen in the following figures, unless specially mentioned.

Note that the parameter η_{total} is not a true efficiency because it will be larger than 1 under some conditions. To compare the case without considering absorption processes, we will also draw figures of the probability that the acceptor is in its excited state, i.e., $P = \text{Tr}[|e\rangle_2\langle e|]$. Generally, the population in the donor pigment should be considered because the population correlates with the whole efficiency. However, in the present studies, the pigment-environment coupling is assumed smaller than the coupling between pigments. There are only resonant and near-resonant frequencies in the pulse to match the eigenstates which overlap with the donor pigment. So we will not consider the population in the donor pigment.

It is also important to study the dynamics of quantum entanglement of typical dimer systems. We choose the concurrence C to quantify the entanglement [42], which is defined $C = \max\{0, \varepsilon_0\}$, and $\varepsilon_0 = \varepsilon_1 - \varepsilon_2 - \varepsilon_3 - \varepsilon_4$, where ε_i are the square roots of the eigenvalues of $\rho\widetilde{\rho}$ in decreasing order, and $\widetilde{\rho} = (\sigma_y \otimes \sigma_y)\rho^*(\sigma_y \otimes \sigma_y)$.

III. THE MASTER EQUATION AND NUMERICAL INVESTIGATION

In the eigenspace and under the second-order approximation of the coupling between the two-level systems and the environment, the master equation is in the following form:

$$\dot{\rho}(t) = -i[H_M(t), \rho(t)] + L\rho(t), \tag{10}$$

where the Lindblad operator is $L\rho(t) = -\sum_{\mu=1}^{12} \xi_\mu (\{\pi_\mu^+ \pi_\mu, \rho(t)\} - 2\pi_\mu \rho(t) \pi_\mu^+)$. The detailed parameters are given by

$$\xi_m = \begin{cases} \epsilon_{ij} \sum_{l=1}^{2} \kappa_k s_{ij}^{(l)} s_{ji}^{(l)} [N_l(\epsilon_{ij}) + 1]; & m \leqslant 6 \\ \epsilon_{ij} \sum_{l=1}^{2} \kappa_k s_{ij}^{(l)} s_{ji}^{(l)} N_l(\epsilon_{ij}); & 7 \leqslant m \leqslant 12 \end{cases}, \tag{11}$$

where ξ_m corresponds to all six level gaps greater than zero: $\epsilon_{21}, \epsilon_{23}, \epsilon_{24}, \epsilon_{31}, \epsilon_{34}$, and ϵ_{41}, respectively, and $\pi_1 = \pi_7^+ = |\epsilon_3(t)\rangle\langle\epsilon_2(t)|$, $\pi_2 = \pi_8^+ = |\epsilon_4(t)\rangle\langle\epsilon_2(t)|$, $\pi_3 = \pi_9^+ = |\epsilon_1(t)\rangle\langle\epsilon_2(t)|$, $\pi_4 = \pi_{10}^+ = |\epsilon_4(t)\rangle\langle\epsilon_3(t)|$, $\pi_5 = \pi_{11}^+ = |\epsilon_1(t)\rangle\langle\epsilon_3(t)|$, $\pi_6 = \pi_{12}^+ = |\epsilon_1(t)\rangle\langle\epsilon_4(t)|$, $N_l(\epsilon_{ij}) = 1/(e^{\epsilon_{ij}/K_B T_l} - 1)$. In the above deduction, the usual Born-Markov approximation and the rotating-wave approximation are performed, and an ohmic spectral density with infinite cut-off frequency is also assumed for the heat bath. To evaluate the dynamic features of the systems under dissipation, we let $\rho_{kl}(t) = \langle\epsilon_i(t)|\rho|\epsilon_i(t)\rangle$ and $X(t) = [\rho_{11}, \rho_{22}, \rho_{33}]^T$, with the relation $\rho_{11} + \rho_{22} + \rho_{33} + \rho_{44} = 1$. Based on these notations, we get the following dynamic equations that denote the process of thermalization:

$$\dot{X}(t) = -M(t)X(t) + R(t), \tag{12}$$

and

$$\dot{\rho}_{kl}(t) = -(\eta_l + \eta_k - i\epsilon_{lk})\rho_{kl}(t), \quad k \neq l, \tag{13}$$

where $R(t) = 2[\xi_9, \xi_{11}, -\xi_{12}]^T$, $\eta_1 = \xi_9 + \xi_{11} + \xi_{12}$, $\eta_2 = \xi_1 + \xi_2 + \xi_3$, $\eta_3 = \xi_4 + \xi_5 + \xi_7$, $\eta_4 = \xi_6 + \xi_8 + \xi_{10}$,

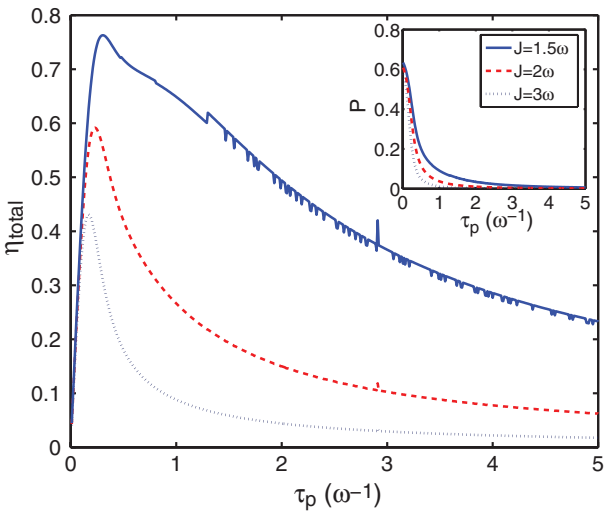

FIG. 2. (Color online) The saturation values of η_{total} and P (inset) with different J versus τ_p are plotted.

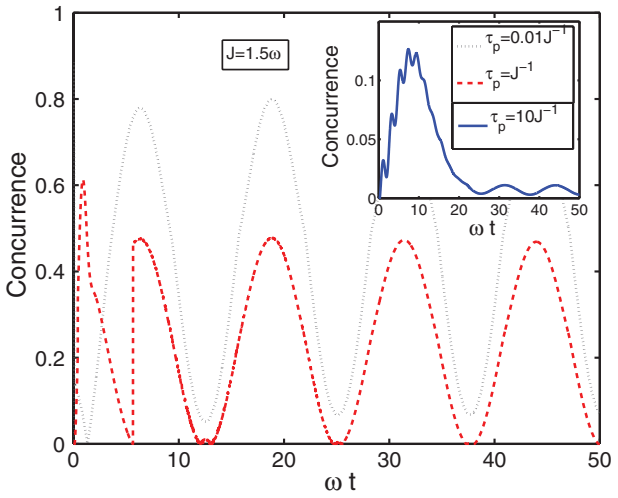

FIG. 3. (Color online) Quantum concurrence between the two pigments versus time ωt are plotted.

and

$$M(t) = 2\begin{bmatrix} \xi_9+\eta_2 & \xi_9-\xi_7 & \xi_9-\xi_8 \\ \xi_{11}-\xi_1 & \xi_{11}+\eta_3 & \xi_{11}-\xi_{10} \\ \xi_{12}-\xi_2 & \xi_{12}-\xi_4 & \xi_{12}+\eta_3 \end{bmatrix}. \quad (14)$$

Based on these equations, we can obtain the elements of the density matrix in the original space:

$$\sigma_{ij} \equiv \mathrm{Tr}[\rho|\eta_j\rangle\langle\eta_i|] = \sum_{k=1}^{4}\sum_{l=1}^{4} u_{jk}u_{il}^{*}\rho_{lk}. \quad (15)$$

In the following section, we will show some numerical results of the dynamical properties of the model based on Eq. (15).

A. Excited by a single Gaussian-type pulse

We first suppose that the input pulse is a Gaussian-type pulse, which has the same form as we mentioned previously. In order to compare the input and output energy in our numerical results, we assume that the amplitude of input pulse is $E_0 = \omega_1$.

In Figs. 1(a) and 1(b), we plot the probability P that the acceptor pigment is in the excited state and the associated η_{total} versus time, respectively. We let $\omega_1 = \omega_2 = \omega$ [43], and set $\omega = 1$ as the calculation unit. The largest width of the pulse is chosen as $\tau_p = 10J^{-1}$ (solid blue line), in which J^{-1} is used to valuate the time scale of state exchange between the two pigments. We set $\tau_p = 0.01J^{-1}$ (solid brown line) to simulate a δ pulse. We find from the figures that both P and η_{total} oscillate with time and approach saturation. For the case that τ_p values are small, oscillation represents that the excited states and excitation energy transfer between the two pigments. But for the case of $\tau_p = 10J^{-1}$, we easily find that the dynamics of P is in connection with the processes of excitation. In the case of inputting a δ pulse, the acceptor is always in the excited states but the dimer has the smallest total efficiency η_{total}, which means that higher probability of the acceptor being in the excited state is not equivalent to successful energy absorbing and transferring in a photochemical reaction process. Figure 2 shows that the saturation values of P are decreasing with increasing τ_p, but there is an optimum of intervals of τ_p for the saturation values of η_{total}.

We also draw the dynamics of quantum concurrence between the two pigments in Fig. 3. We observe from the figures that quantum entanglement can be produced in the dimer when the donor is excited by a pulse, and find that a shorter temporal pulse will induce larger entanglement.

B. Excited by sequential Gaussian-type pulses

In the above, we have studied the dynamics of a dimer being excited by a single Gaussian pulse. In order to understand

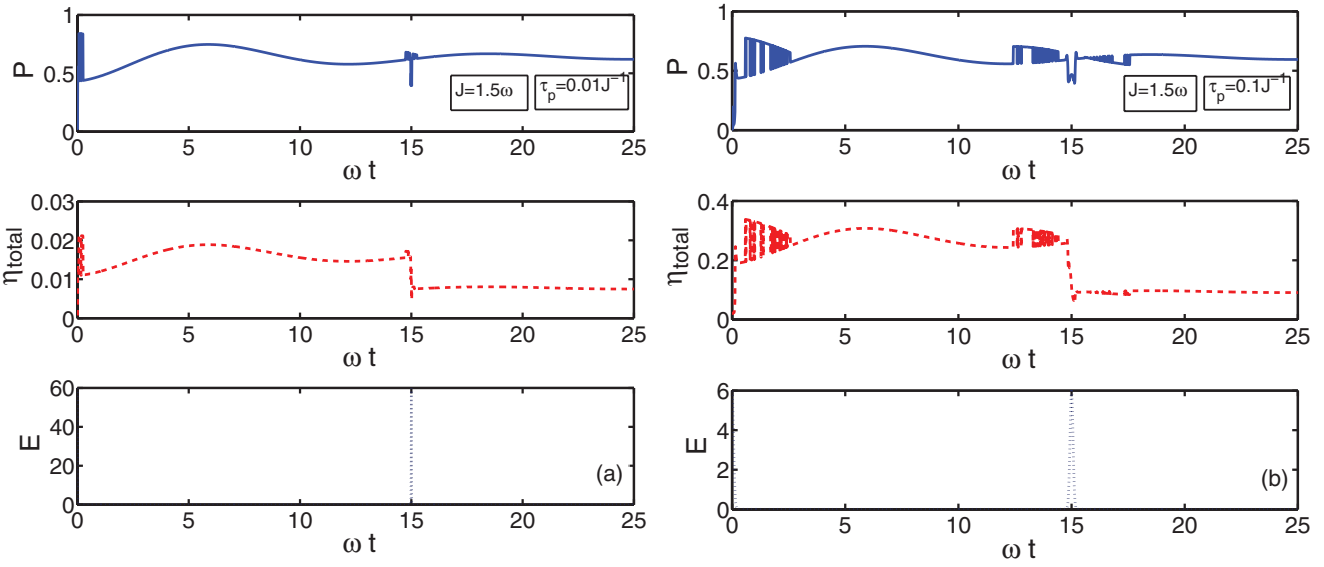

FIG. 4. (Color online) Probability P that the acceptor is in the excited state and the parameter of total efficiency η_{total} versus time ωt are plotted. We set the width of the pulse at $\tau_p = 0.01J^{-1}$ and $\tau_p = 0.1J^{-1}$ in (a) and (b), respectively.

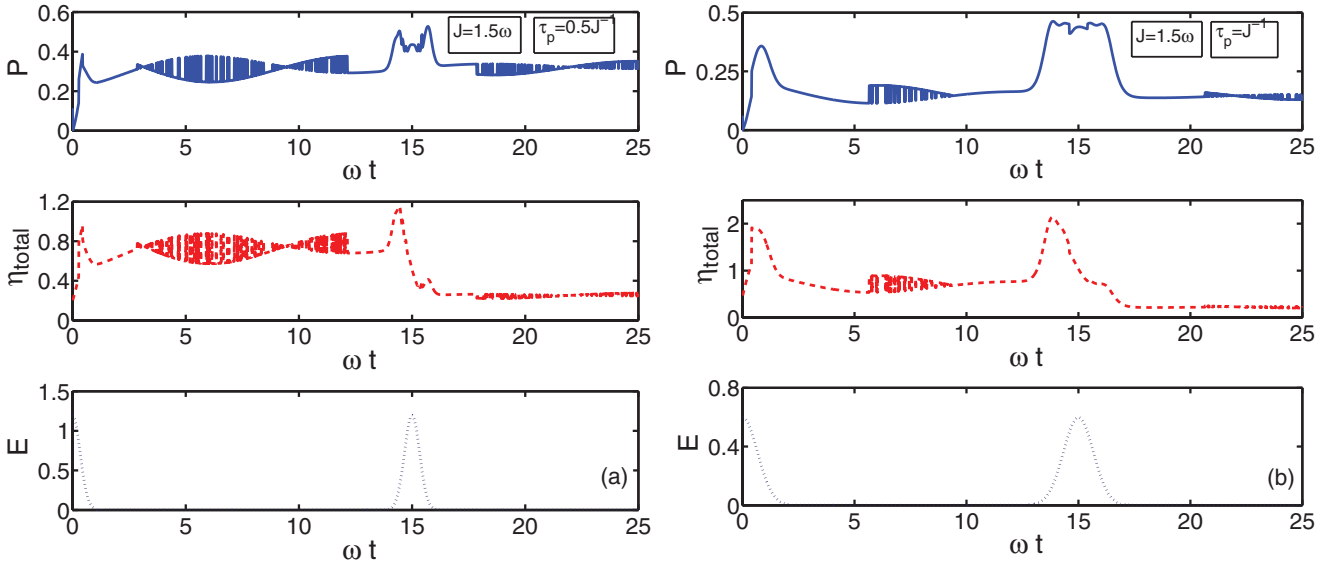

FIG. 5. (Color online) Probability P that the acceptor is in the excited state and the parameter of total efficiency η_{total} versus time ωt are plotted. We set the width of pulses as $\tau_p = 0.5J^{-1}$ and $\tau_p = J^{-1}$ in (a) and (b), respectively.

how temporal properties of an input pulse affect the quantum dynamics of the dimer, we now consider some more complex cases.

In the figures from Fig. 4(a) to Fig. 6(a), we consider the case that the donor pigment is excited sequentially by two of the same Gaussian-type pulses. The central time of the first pulse is $\omega t = 0$, and the central time of the second pulse is $\omega t = 15$. In Figs. 4(a) and Fig. 4(b), we set the width of the pulse at $\tau_p = 0.01$ and $0.1J^{-1}$, respectively. We find that in both cases, compared with the associated Figs. 1(a) and 1(b), the probability P has only a sharp slip down during the second acting pulse, and η_{total} has a sudden decrease. However, when we set $\tau_p = 0.5J^{-1}$ and $\tau_p = \text{J}^{-1}$ in Figs. 5(a) and Fig. 5(b), respectively, we find contrary phenomena, i.e., the probability P has an upward change during the second pulse turning on and similar changes to η_{total}, decreasing finally. There should be two physical mechanisms to understand the phenomena in Figs. 4 and 5. In the first aspect, we observe that probability P is always larger than 0.5 when the second pulse is absent in the cases of $\tau_p = 0.01$ and $0.1J^{-1}$, which means that the acceptor pigment is always in its excited state after the first pulse acting on, so the second pulse will induce stimulated radiation with larger probability than that of stimulated absorption. Second, one need also note the fact that excited-state absorption can also deplete the population in the single exciton manifold (i.e., population in the acceptor). This means that the coherent effects from the sequential multipulses in the acceptor pigment take place during a short time scale,

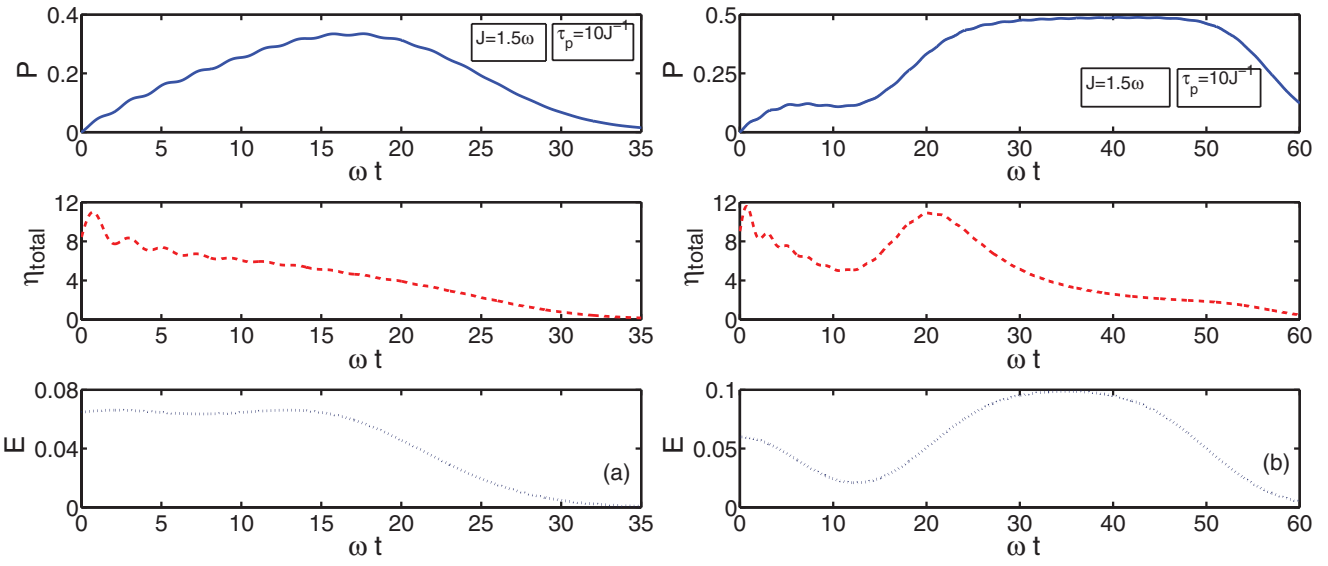

FIG. 6. (Color online) Probability P that the acceptor is in the excited state and the parameter of total efficiency η_{total} versus time ωt are plotted. In Fig. 6(b), four sequential pulses are initiated on the donor pigment, the width of pulses are all $\tau_p = 10J^{-1}$, and the central action times are $\omega t = 0, 25, 35,$ and 45, respectively.

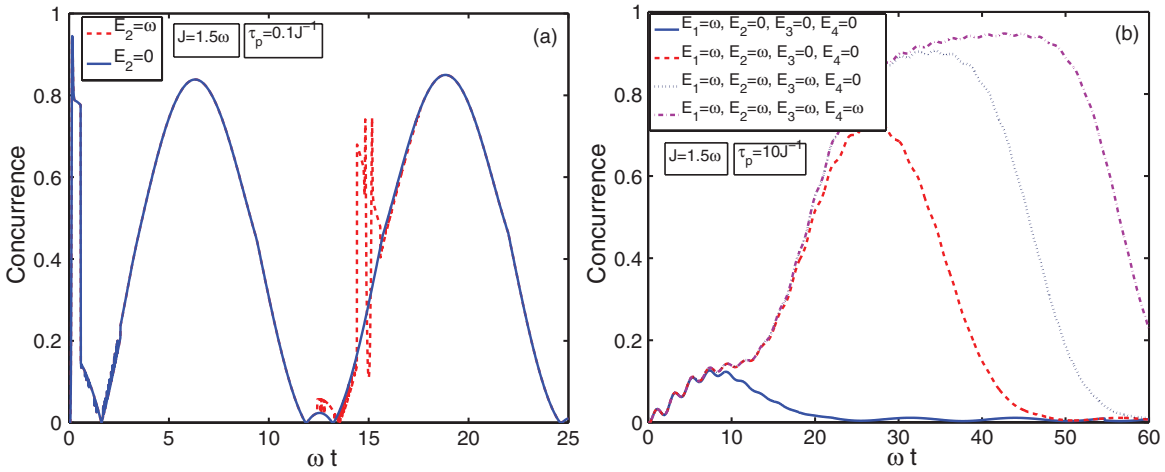

FIG. 7. (Color online) Quantum concurrence between the two pigments versus time ωt are plotted. In Fig. 7(b), four pulses are turned on sequentially, the width of pulses are all $\tau_p = 10J^{-1}$, and the central action times are $\omega t = 0,25,35,$and 45, respectively.

and thus deplete population. It will induce contrary results in the cases of $\tau_p = 0.5J^{-1}$ and $\tau_p = \mathrm{J}^{-1}$, because the probability P is always smaller than 0.5.

In Fig. 6(a), we set $\tau_p = 10J^{-1}$ and produce a near-constant pulse during times from $\omega t = 0$ to $\omega t = 15$, which makes a continuous enhancement of probability P compared with Fig. 1(a), but the total efficiency η_{total} decreases at all times. In Fig. 6(b), we show the case that four sequential pulses are initiated on the dimer, widths of pulses are all $\tau_p = 10J^{-1}$, and the central action times are $\omega t = 0,25,35,$ and 45, respectively. We increase the time intervals of the first and the second pulses to $25\omega t$ and produce a near constant P during ωt =25–50, by which we realize controlling populations of the acceptor pigment simply by adjusting the temporal shapes of the input pulses. We also obtain an extreme value of η_{total} near $\omega t = 20$. But as we have mentioned previously, the values of P are always not larger than 0.5.

Finally, we plot quantum concurrence between the two pigments when the donor pigment is excited by multipulses sequentially. In Fig. 7(a), we consider the case where two sequential pulses are applied, where the central time of the first pulse is at $\omega t = 0$, the central time of the second pulse is at $\omega t = 15$, and $\tau_p = 0.1J^{-1}$. We find there is only a disturbance of quantum concurrence when the second pulse is turned on. However, in Fig. 7(b), quantum concurrence is largely enhanced when the second pulse, the third pulse, and the fourth pulse turn on sequentially, where we set $\tau_p = 10J^{-1}$ and the central times of the four pulses are the same as those shown in Fig. 6(b). Compared with the results shown in Figs. 4 and 5, where the probability P can only be enhanced to a maximum value 0.5, we find quantum concurrence can be enhanced to very large values. This is because quantum coherence between the two pigments can be continuously induced, no matter whether the system is in the processes of stimulated emission or stimulated absorption.

IV. CONCLUSIONS

In summary, we have studied controlling excitation and coherent transfer in a dimer. In our model, energy transferring from the donor to the acceptor takes place during processes where the donor is being excited. The model can be applied to find a physical mechanism of the basic processes of energy absorption and transfer for photosynthesis. We mainly investigated how temporal shapes of the input pulses affect the population behavior of the acceptor and quantum concurrence of the dimer. We find a high probability of the acceptor being excited can be obtained with very sharp pulses but with a very low total efficiency of energy absorption and transfer. The total efficiency depends on the temporal shape of the input pulses. When the dimer is excited by sequential multipulses, there are two physical mechanisms to determine the probability of the acceptor being excited. One is the coherent effects from the sequential multipulses in the acceptor pigment during a short timescale, and another is the population conditions of the acceptor before being pumped again, i.e., the later pulses will induce the acceptor pigment being stimulated emission or stimulated absorption. Our results also show that a high degree of quantum concurrence of the dimer can be obtained by controlling the temporal shape of the input pulses. Our studies may contribute to the fundamental research of artificial photosynthetic units.

ACKNOWLEDGMENTS

This work is supported by the National Natural Science Foundation of China (Grants No. 11174233 and No. 11004158), the Special Prophase Project on the National Basic Research Program of China (Grant No. 2011CB311807), and the Fundamental Research Funds for the Central Universities.

[1] R. E. Blankenship, *Molecular Mechanisms of Photosynthesis* (World Scientific, London, 2002).
[2] G. R. Fleming and R. V. Grondelle, Phys. Today **47**, 48 (1994).
[3] X. Hu and K. Schulten, Phys. Today **50**, 28 (1997).
[4] V. I. Novoderezhkin, M. A. Palacios, H. van Amerongen, and R. van Grondelle, J. Phys. Chem. B **108**, 10363 (2004).

[5] M. Cho, H. M. Vaswani, T. Brixner, J. Stenger, and G. R. Flemming, J. Phys. Chem. B **109**, 10542 (2005).
[6] J. Adolphs and T. Renger, Biophys. J. **91**, 2778 (2006).
[7] J. Savolainen, R. Fanciulli, N. Dijkhuizen, A. L. Moore, J. Hauer, T. Buckup, M. Motzkus, and J. L. Herek, Proc. Natl. Acad. Sci. USA **105**, 7641 (2008).
[8] T. Brixner, J. Stenger, H. M. Vaswani, M. Cho, R. E. Blankenship, and G. R. Fleming, Nature (London) **434**, 625 (2005).
[9] R. E. Fenna and B. Matthews, Nature (London) **258**, 573 (1975).
[10] T. Forster, Ann. Phys. **437**, 55 (1948).
[11] S. I. E. Vulto, M. A. de Baat, S. Neerken, F. R. Nowak, H. van Amerongen, J. Amesz, and T. J. Aartsma, J. Phys. Chem. B **103**, 8153 (1999).
[12] A. Ishizaki and G. R. Fleming, J. Chem. Phys. **130**, 234111 (2009).
[13] G. S. Engel, T. R. Calhoun, E. L. Read, T.-K. Ahn, T. Mancal, Y.-C. Cheng, R. E. Blankenship, and G. R. Fleming, Nature (London) **446**, 782 (2007).
[14] H. Lee, Y.-C. Cheng, and G. R. Fleming, Science **316**, 1462 (2007).
[15] E. Collini and D. Scholes, Science **323**, 369 (2009).
[16] I. P. Mercer, Y. C. El-Taha, N. Kajumba, J. P. Marangos, J. W. G. Tisch, M. Gabrielsen, R. J. Cogdell, E. Springate, and E. Turcu, Phys. Rev. Lett. **102**, 057402 (2009).
[17] E. Collini, C. Y. Wong, K. E. Wilk, P. M. G. Curmi, P. Brumer, and G. D. Scholes, Nature (London) **463**, 644 (2010).
[18] A. Olaya-Castro, C. F. Lee, F. F. Olsen, and N. F. Johnson, Phys. Rev. B **78**, 085115 (2008).
[19] M. B. Plenio and S. F. Huelga, New J. Phys. **10**, 113019 (2008).
[20] M. Mohseni, P. Rebentrost, S. Lloyd, and A. A.-Guzik, J. Chem. Phys. **129**, 174106 (2008).
[21] P. Rebentrost, M. Mohseni, I. Kassal, S. Lloyd, and A. Aspuru-Guzik, New J. Phys. **11**, 033003 (2009).
[22] F. Caruso, A. W. Chin, A. Datta, S. F. Huelga, and M. B. Plenio, J. Chem. Phys. **131**, 105106 (2009).
[23] J. S. Cao and R. J. Silbey, J. Phys. Chem. A **113**, 13825 (2009).
[24] A. Nazir, Phys. Rev. Lett. **103**, 146404 (2009).
[25] M. Thorwart, J. Eckel, J. H. Reina, P. Nalbach, and S. Weiss, Chem. Phys. Lett. **478**, 234 (2009).
[26] M. Sarover, A. Ishizaki, G. R. Fleming, and K. B. Whaley, Nat. Phys. **6**, 462 (2010).
[27] G. Panitchayangkoon, D. Hayes, K. A. Fransted, J. R. Caram, E. Harel, J. Wen, R. E. Blankenship, and G. S. Engel, Proc. Natl. Acad. Sci. USA **107**, 12766 (2010).
[28] S. Yang, D. Z. Xu, Z. Song, and C. P. Sun, J. Chem. Phys. **132**, 234501 (2010).
[29] F. Caruso, A. W. Chin, A. Datta, S. F. Huelga, and M. B. Plenio, Phys. Rev. A **81**, 062346 (2010).
[30] T. Mancal and L. Valkunas, New J. Phys. **12**, 065044 (2010).
[31] F. Fassioli and A. Olaya-Castro, New J. Phys. **12**, 085006 (2010).
[32] J.-Q. Liao, J.-F. Huang, L.-M. Kuang, and C. P. Sun, Phys. Rev. A **82**, 052109 (2010).
[33] D. P. S. McCutcheon and A. Nazir, Phys. Rev. B **83**, 165101 (2011).
[34] P. K. Ghosh, A. Yu. Smirnov, and F. Nori, Phys. Rev. E **84**, 061138 (2011).
[35] J. S. Briggs and A. Eisfeld, Phys. Rev. E **83**, 051911 (2011); A. Eisfeld and J. S. Briggs, *ibid.* **85**, 046118 (2012).
[36] F. Caruso, S. K. Saikin, E. Solano, S. F. Huelga, A. Aspuru-Guzik, and M. B. Plenio, Phys. Rev. B **85**, 125424 (2012); F. Caruso, S. Montangero, T. Calarco, S. F. Huelga, and M. B. Plenio, Phys. Rev. A **85**, 042331 (2012).
[37] M. Allegra and P. Giorda, Phys. Rev. E **85**, 051917 (2012).
[38] A. Shabani, M. Mohseni, H. Rabitz, and S. Lloyd, Phys. Rev. E **86**, 011915 (2012).
[39] L. A. Pachon and P. Brumer, Phys. Rev. A **87**, 022106 (2013).
[40] J. Yuen-Zhou and A. Aspuru-Guzik, J. Chem. Phys. **134**, 134505 (2011).
[41] J. Yuen-Zhou, J. J. Krich, M. Mohseni, and A. Aspuru-Guzik, Proc. Nat. Acad. Sci. USA **108**, 17615 (2011).
[42] S. Hill and W. K. Wootters, Phys. Rev. Lett. **78**, 5022 (1997); W. K. Wootters, *ibid.* **80**, 2245 (1998).
[43] We also studied the case of $\omega_1 \neq \omega_2$, and found the same main results with the present case.